

## Synthesis and Characterization of Magnetic Nanoparticle ( $\text{Fe}_3\text{O}_4$ ) and its Impregnated onto Rice Husk Ash ( $\text{Fe}_3\text{O}_4$ )/RHA

Khant Nyar Oo<sup>1</sup>, Soe Zar Zar Nwe<sup>1</sup>, Sandar Aung<sup>1</sup>, Aung Phyto Kyaw<sup>2</sup>, Hlaing Hlaing Myint<sup>3\*</sup>

<sup>1</sup>Department of Chemistry, Meiktila University, Mandalay, Myanmar, 05181, <sup>2</sup>Department of Chemistry, Shwe Bo University, Shwe Bo, Myanmar, 02231, <sup>3</sup>Department of Chemistry, Monywa University, Monywa, Myanmar, 02301

### ABSTRACT

The aim of this study was to develop synthetic magnetite nanoparticles ( $\text{Fe}_3\text{O}_4$ ) and its impregnated onto rice husk ash for possible environmental applications as adsorbents. The synthetic magnetite – nanoparticles (MNP –  $\text{Fe}_3\text{O}_4$ ) obtained through the chemical coprecipitation of both  $\text{Fe}^{2+}$  and  $\text{Fe}^{3+}$  ions ( $\text{Fe}^{2+}/\text{Fe}^{3+} = 2:3$  ratio). The resulting particles were characterized by Fourier-transform infrared spectroscopy, UV visible spectrophotometer, and X-ray diffraction spectrophotometer.  $\text{Fe}_3\text{O}_4$  displayed a wide specific surface area ( $160 \text{ m}^2 \text{ g}^{-1}$ ) with particles reaching a size of about 27 nm and its impregnated ones ( $\text{Fe}_3\text{O}_4$ /RHA) estimated at 17 nm while showing a surface area of  $179 \text{ m}^2 \text{ g}^{-1}$ . The magnetization measurements, at room temperature, showed that the particles are in the superparamagnetic regime. Magnetite was also synthesized in acid solutions in basic environment (26% ammonia solution), a medium that allows to proceed by the chemical coprecipitation process in two step reaction. The superparamagnetic behavior is preserved, although its saturation is probably due to the contribution of the smallest particles.

**Key words:** Magnetite, Impregnated, Coprecipitation method, Superparamagnetic, Rice husk ash.

### 1. INTRODUCTION

Magnetic nanoparticles (MNPs) ( $\text{Fe}_3\text{O}_4$ ) become the study focus of material scientists due to their unique physicochemical and high application potentials such as magnetic data storage, environmental remediation, catalyst, sensor, and biomedical field. Moreover, the application of MNPs ( $\text{Fe}_3\text{O}_4$ ) in the field of wastewater treatment is becoming an interesting area of research, because it exhibits good adsorption efficiency especially due to higher surface area and greater active sites for interaction with metallic species and can easily be synthesized; several research have used it as an adsorbent [1]. In general, there are various methods for synthesizing  $\text{Fe}_3\text{O}_4$  MNPs. Among the various methods, the chemical coprecipitation method is a facile and convenient approach method to synthesis MNPs such as  $\text{Fe}_3\text{O}_4$  which is easy to do with the success rate from 96% to 99.9% [2]. The advantages of the coprecipitation method are the high yield, high product purity, the lack of necessity to use organic solvents, easily reproducible, and low cost. Chemical coprecipitation can produced fine, stoichiometry particles of single and multi-component metal oxides [3]. The common way of magnetite synthesis is the alkaline hydrolysis of Fe (II) and Fe (III)-salts. Other advantages of the magnetic  $\text{Fe}_3\text{O}_4$  nanoparticles, including scalable and non-toxic synthesis and eco the main potential adsorbent for toxic and radioactive heavy metals. Moreover, burning agricultural waste has been a prevalent cause of environmental concern, especially in developing countries. In this study, the raw material (rice husk ash) used to synthesize  $\text{Fe}_3\text{O}_4$  because rice husk is an abundantly available agricultural waste has emerged as an ideal source of high-grade amorphous silica. Many studies have been reported on the use of silica from rice husk as a catalyst support. Magnetic rice husk ash (MRHA) was highly stable and reusable and had its high potential as an economical. MRHA has a higher surface area and mesopore volume compared to RHA possibly caused by the presence of ferrite nanoparticles which are known to have a large surface area and pore volume [4-6]. In this research, the synthesis and characterization of the (MNP,  $\text{Fe}_3\text{O}_4$ )

and impregnated onto rice husk ash  $\text{Fe}_3\text{O}_4$ /RHA was studied. This research was divided into two phases: one phase was preparation of MNPs and MNPs impregnated onto the rice husk ash and second phase was characterization of these samples. The physicochemical analysis of MNPs ( $\text{Fe}_3\text{O}_4$ ) and MNPs impregnated onto the rice husk ash ( $\text{Fe}_3\text{O}_4$ /RHA) was characterized by Fourier-transform infrared spectroscopy (FTIR), UV-vis spectrophotometer scanning electron microscopy (SEM), and X-ray diffraction spectrometer (XRD). Finally, this research can be applied for possible application of technological applications, such as a catalyst for ammonia, ceramics, energy storage, magnetic data storage, ferrofluids, and bioapplications.

### 2. EXPERIMENTAL

#### 2.1. Materials

Ferric chloride ( $\text{FeCl}_3 \cdot 6\text{H}_2\text{O}$ ), ferrous sulfate ( $\text{FeSO}_4 \cdot 7\text{H}_2\text{O}$ ), ammonium hydroxide ( $\text{NH}_4\text{OH}$ ), and distilled water were used.

#### 2.2. Sample Collection and Preparations

The rice husk used in this study was collected from a rice processing factory in the Ingyinkan village Yamethin Township Mandalay Region, Myanmar. Raw rice husks were washed with a stream of distilled water

#### \*Corresponding author:

Hlaing Hlaing Myint,

E-mail: hlainghlaingmyint80@gmail.com

ISSN NO: 2320-0898 (p); 2320-0928 (e)

DOI: 10.22607/IJACS.2023.1101003

Received: 11<sup>th</sup> December 2022;

Revised: 22<sup>th</sup> December 2022;

Accepted: 25<sup>th</sup> December 2022

to remove dirt, dust, and superficial impurities and then dried in an oven at 105°C for 24 h. Rice husks were carbonized in air in a muffle furnace (NUVE MF120) at 500°C for 45 min and cooled to room temperature.

### 2.3. Preparation of MNPs of Fe<sub>3</sub>O<sub>4</sub> and its Impregnated onto Rice Husk Ash (Fe<sub>3</sub>O<sub>4</sub>/RHA)

Fe<sub>3</sub>O<sub>4</sub> magnetic nanoparticles were prepared by chemical coprecipitation method. 4.2 g of FeSO<sub>4</sub>·7H<sub>2</sub>O and 6.1 g of FeCl<sub>3</sub>·6H<sub>2</sub>O were dissolved in 100 mL of distilled water and heated up to 90°C for 30 min with stirring. After that, 10 mL 26% of ammonium hydroxide was added to each other quickly. pH was adjusted to 10. The mixture was mixed for 30 min at 80°C and cooled down at room temperature for 5 min. The obtained MNPs (MNP-Fe<sub>3</sub>O<sub>4</sub>) was left for the settlement for 30 min. It was filtered and then washed with distilled water until neutral. After that, the obtained paste MNP-Fe<sub>3</sub>O<sub>4</sub> was dried at 50°C for 6 h. The reaction that occurs in the production of MNPs is shown in equation (1). The same procedure of Fe<sub>3</sub>O<sub>4</sub> and its impregnated onto rice husk ash (Fe<sub>3</sub>O<sub>4</sub>/RHA) was synthesized. Fe<sub>3</sub>O<sub>4</sub> nanoparticle was added into the solution of 1 g rice husk ash (RHA) with 200 mL of distilled water. The mixture was adjusted to pH 10. The mixture was mixed for 2 h at 80°C under constant stirring. The resulting suspension of MNPs (Fe<sub>3</sub>O<sub>4</sub>/RHA) was left for the settlement to cool to room temperature for 5 min. Moreover, it was washed with distilled water until the neutral condition to get rid of excess and unreacted chemicals. Filtered MNP/RHA was oven dried at 50°C for 6 h. The reaction that occurs in the production of MNPs and Fe<sub>3</sub>O<sub>4</sub> and its impregnated onto rice husk ash Fe<sub>3</sub>O<sub>4</sub>/RHA is shown in equation (2).



### 2.4. Determination of Surface and Crystallite Sizes of Fe<sub>3</sub>O<sub>4</sub> and Fe<sub>3</sub>O<sub>4</sub>/RHA

The surface area and crystallite sizes are most assumed to be important property of any material and can disclose imperative information. Therefore, this research investigated the surface area and crystallite sizes were calculated using Sear's equation (3) and Debye Scherrer equation (4).

According to Sear's Equation,

$$A = 32. V - 25 \quad (3)$$

where, A = Surface area of samples per gram (in m<sup>2</sup>/g)

V = volume of 0.1N NaOH required to raise the pH from 4 to 9.

According to Debye Scherrer Equation,

$$D = \frac{K\lambda}{\beta \cos\theta} \quad (4)$$

where, D = average particle size in nm (or) Å°

λ = wavelength of X-ray Å° (or) nm

K = Dimensionless shape factor (0.9)

β = FWHM (full width at half maximum of the sharp peaks)

## 3. RESULTS AND DISCUSSION

### 3.1. Determination of Magnetic Properties of Fe<sub>3</sub>O<sub>4</sub> and Fe<sub>3</sub>O<sub>4</sub>/RHA in Aqueous Medium

The superparamagnetic behavior of Fe<sub>3</sub>O<sub>4</sub> and its impregnated onto rice husk ash is verified using an external magnet in water, as shown in Figure 1a and b.

The superparamagnetic behavior of Fe<sub>3</sub>O<sub>4</sub> and Fe<sub>3</sub>O<sub>4</sub>/RHA had remained

intact which can be easily recovered after their application in the aqueous medium. The separation and redispersing process of the Fe<sub>3</sub>O<sub>4</sub> and Fe<sub>3</sub>O<sub>4</sub>/RHA was investigated. In the absence of an external magnetic field, the dispersion of the Fe<sub>3</sub>O<sub>4</sub> and (b) Fe<sub>3</sub>O<sub>4</sub>/RHA nanoparticles was settled back and homogenous. The Fe<sub>3</sub>O<sub>4</sub> NPs and Fe<sub>3</sub>O<sub>4</sub>/RHA were separated and purified from solvent by a magnet for several times. A black precipitation was obtained and then redissolved in water by an orbital shaker several minutes. This indicates that the magnetite nanoparticles are highly soluble in water to form a stable ferrofluid suspension. Particles were dispersed in water solution and orbital shaker to achieve colloidal stability [7]. When the external magnetic field was applied, Fe<sub>3</sub>O<sub>4</sub> and Fe<sub>3</sub>O<sub>4</sub>/RHA nanoparticles were enriched leading to transparency of the dispersion. The results confirmed that the formation of Fe<sub>3</sub>O<sub>4</sub>/RHA nanoparticles and the Fe<sub>3</sub>O<sub>4</sub> possessed superparamagnetic properties. The surface area of the Fe<sub>3</sub>O<sub>4</sub> was impregnated on rice husk ash (Fe<sub>3</sub>O<sub>4</sub>/RHA) which played an important role in restraining the aggregation of MNPs and enhancing their dispersion and colloidal stability.

### 3.2. SEM measurements of RHA, Fe<sub>3</sub>O<sub>4</sub>, and Fe<sub>3</sub>O<sub>4</sub>/RHA

In SEM spectrometer, the surface of the specimen was analyzed by an electron beam. The morphological structure of sample (RHA, Fe<sub>3</sub>O<sub>4</sub>, and Fe<sub>3</sub>O<sub>4</sub>/RHA) was studied the roughness and smoothness of their surface in (Figures 2-4). The micrographs obtained from SEM gave a highly magnified image on the surface of a material and the adsorbents surface was irregular, rough, and highly porous, indicating the possibility of its good adsorption properties, in which it occurs in the RHA is already a wide distribution of sizes in the nano-range, which is <100 nm in Figure 2.

The SEM micrographs of Fe<sub>3</sub>O<sub>4</sub> particles were synthesized using the coprecipitation method. The average size of these nanoparticles is about 27 nm dense morphology for all samples with a uniform distribution of

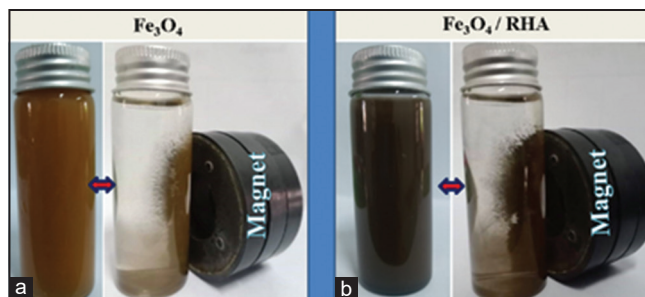


**Figure 1:** Photographs of a vial containing (a) Fe<sub>3</sub>O<sub>4</sub> and (b) Fe<sub>3</sub>O<sub>4</sub>/RHA in aqueous dispersion when a magnet was attached to the outside of the sample vial.

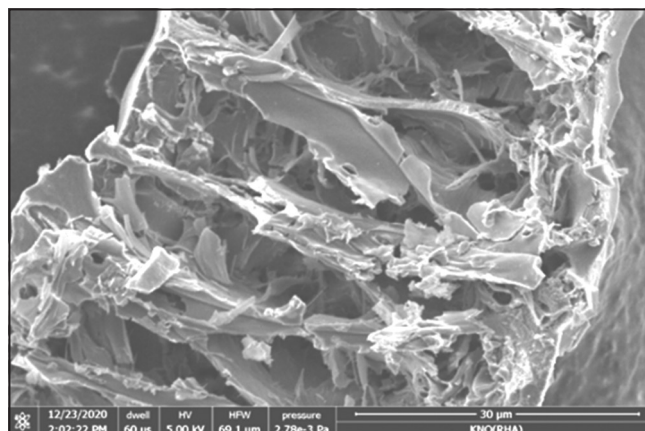


**Figure 2:** SEM micrograph of rice husk ash (RHA).



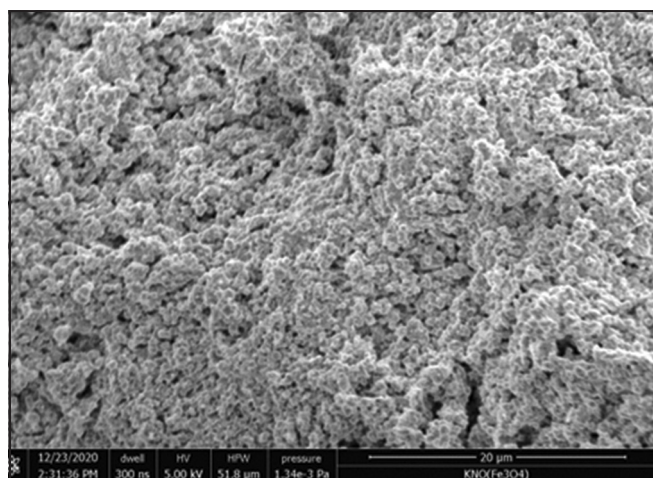


Figure 3: SEM micrograph of  $\text{Fe}_3\text{O}_4$ .

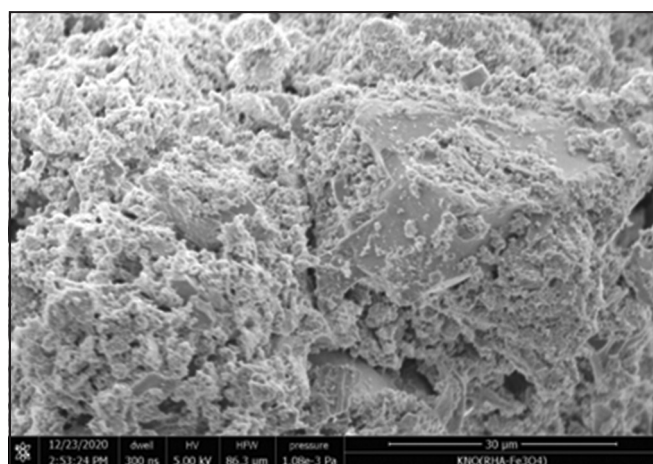


Figure 4: SEM micrograph of  $\text{Fe}_3\text{O}_4/\text{RHA}$ .

spherical particles indicated that the aggregation of the nanoparticles is shown clearly in Figure 3.

Figure 4 shows the SEM image of the ( $\text{Fe}_3\text{O}_4/\text{RHA}$ ). It showed that the particles were homogeneously distributed without any substantial agglomeration. The modified surface of magnetite particles with suitable and non-toxic compounds has been proven to be one of the most efficient ways for providing stability of the nanoparticles. On the other hand, agglomeration of impregnated  $\text{Fe}_3\text{O}_4$  NPs was reduced due to surface modification.

### 3.3. Characterization of RHA, $\text{Fe}_3\text{O}_4$ , and $\text{Fe}_3\text{O}_4/\text{RHA}$ by FT IR

The Fourier-transform infrared spectrometer (IR-Tracer 100 Shimadzu, Japan) was used to examine the significant absorption spectra due to the stretching, bending, and vibration of the various types of chemical bonding present in RHA,  $\text{Fe}_3\text{O}_4$ , and  $\text{Fe}_3\text{O}_4/\text{RHA}$ , as shown in Figure 5a-c. FT IR spectra of RHA were used to investigate the presence of functional groups in the samples from the obtained vibrational (transmittance/absorption) spectra. This analysis was based on the vibrational excitation of molecular bonds by absorption of infrared light energy within the wavelength from 4000 to 600  $\text{cm}^{-1}$ .

The peaks appear near at 1064  $\text{cm}^{-1}$  is due to the stretching vibration of the C-O bonds. The FTIR spectrum of RHA at 790  $\text{cm}^{-1}$  is attributed to the stretching vibration for Si-O-Si group due to the calcination. In addition, the changes in peaks ranges of  $\text{Fe}_3\text{O}_4$  were observed at 1064  $\text{cm}^{-1}$  and 794  $\text{cm}^{-1}$  which were indicative of stretching vibration

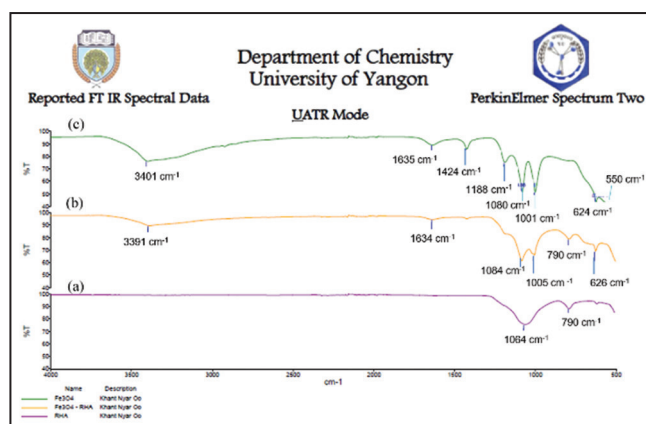


Figure 5: FTIR spectra of (a) RHA, (b)  $\text{RHA}/\text{Fe}_3\text{O}_4$ , and (c)  $\text{Fe}_3\text{O}_4$ .

for C-N and C-H bonds of alcohol group and aromatics group [7,8]. The bands at 1635  $\text{cm}^{-1}$  and 1084  $\text{cm}^{-1}$  are assigned to N-H bending vibration from alkali solution of  $\text{NH}_4\text{OH}$  processing method. The peaks in 624 and 550  $\text{cm}^{-1}$  are observed corresponding to inherent stretching vibrations of metal-oxygen absorption band (Fe-O bonds) in the crystalline lattice of  $\text{Fe}_3\text{O}_4$  at tetrahedral site. In addition, the FTIR peak or absorption bond of  $\text{Fe}_3\text{O}_4$ -RHA which has the range of 550–600  $\text{cm}^{-1}$  is also observed corresponding to inherent stretching vibrations of metal-oxygen at tetrahedral site (Fe tetra-O) [7]. All the spectra were normalized to the intensity of iron oxides Fe-O peak at 548  $\text{cm}^{-1}$  to compare the intensity of peaks at different spectra regions for various adsorbed molecules. Moreover, the peaks in the region numbers 438–575  $\text{cm}^{-1}$  are also attributed to the Fe-O vibration. The band at 1634  $\text{cm}^{-1}$  is assigned to N-H bending vibration that confirms the alkaline solution of ammonium hydroxide and is in good agreement with previous reports [9]. FTIR spectra of 1005  $\text{cm}^{-1}$  are due to Si-O stretching of hydroxyl group and also assigned that the H-O-H bending vibration at about 1000-1600  $\text{cm}^{-1}$ , typical of the  $\text{H}_2\text{O}$  molecule is less intense. The presence of two strong absorption bands at around 626  $\text{cm}^{-1}$  shows the formation of MNPs [14]. Bands at 1084  $\text{cm}^{-1}$  were due to symmetric and asymmetric linear vibrations of Si-O-Si, indicative of the formation of a silica shell with  $\text{SiO}_2$  from rice husk ash impregnated with magnetite  $\text{Fe}_3\text{O}_4$ , and its data supports the formation of  $\text{SiO}_2$  shell on  $\text{Fe}_3\text{O}_4$  transmittance of impregnated  $\text{Fe}_3\text{O}_4$  NPs was slightly lower than that of  $\text{Fe}_3\text{O}_4$  NPs due to the impregnating. The frequencies at 905  $\text{cm}^{-1}$  and 1005  $\text{cm}^{-1}$  are due to Si-O stretching of hydroxyl group.

### 3.4. Characterization of RHA, $\text{Fe}_3\text{O}_4$ , and $\text{Fe}_3\text{O}_4/\text{RHA}$ by XRD

The XRD was a non-destructive analytical technique which can yield the unique fingerprint of reflections associated with a crystal structure. X-ray with a wavelength similar to the distances between these planes can be reflected such that the angle of reflection is equal to the angle of incidence. The XRD patterns of RHA,  $\text{Fe}_3\text{O}_4$ , and  $\text{Fe}_3\text{O}_4/\text{RHA}$  by XRD are shown in Figure 6.

XRD patterns of RHA,  $\text{Fe}_3\text{O}_4$ , and  $\text{Fe}_3\text{O}_4/\text{RHA}$  are shown in Figure 6. The XRD pattern of  $\text{Fe}_3\text{O}_4$  nanoparticles shows six characteristic peaks for  $2\theta$  values of 29.56°, 35.45°, 43.29°, 53.36°, 57.28°, 57.24°, and 62.84° corresponding to 220, 311, 400, 422, 511, and 440 lattice planes and also result was well-matched with the synthesis of magnetite nanoparticle, as shown in Figure 6a. All XRD patterns had a diffraction peak at  $2\theta=35.45^\circ$  corresponding to the spinel phase of the synthesized ( $\text{Fe}_3\text{O}_4$ ) nanoparticles or bulk. After impregnating of RHA on  $\text{Fe}_3\text{O}_4$ , the decrease in the intensity after the diffraction peaks at  $2\theta=35.45^\circ$  could be attributed to

the formulation of more crystalline phase particles in all annealed magnetic ( $\text{Fe}_3\text{O}_4$ ) nanoparticles. The results revealed that good agreement with the XRD standard for the MNPs was observed in the XRD pattern, indicating that the synthesized particles powders are MNPs. After impregnating with rice husk ash, MNPs of  $\text{Fe}_3\text{O}_4$  is retained. A similar peak of  $\text{Fe}_3\text{O}_4/\text{RHA}$  was seen in the XRD in Figure 6b confirming that the intensity of the diffraction peaks is not weakened, which might be due to the still a little high magnetic content and the rice husk ash. Meanwhile, the weak peak at around ( $2\theta = 36^\circ$ ) becomes broad and clear for the  $\text{Fe}_3\text{O}_4/\text{RHA}$  impregnated forms, arising from both of characteristic peak of rice husk ash and  $\text{Fe}_3\text{O}_4$ , which is identified in Figure 6b. However, due to the low concentration of rice husk ash, the amorphous peak is very weak. The XRD patterns further reveal that the  $\text{Fe}_3\text{O}_4/\text{RHA}$  consists of both  $\text{Fe}_3\text{O}_4$  and rice husk ash. This observation is consistent with the obtained findings of the previously performed research in this regard. Sharp XRD peaks at  $2\theta$  values of  $21.95^\circ$  and  $36.02^\circ$  indicates silica in crystalline form from rice husk ash that can be assigned to (101) and (200) form Figure 6c [10].

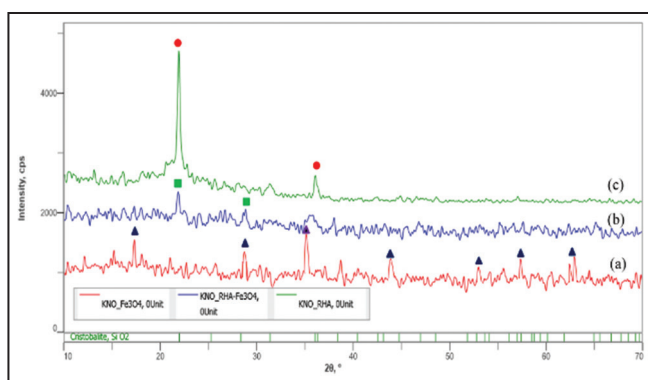


**Figure 6:** XRD patterns of (a)  $\text{Fe}_3\text{O}_4$ , (b)  $\text{Fe}_3\text{O}_4/\text{RHA}$ , and (c) RHA.

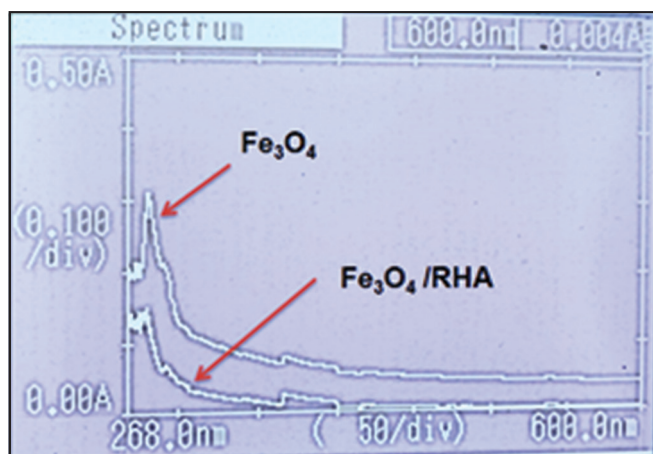


**Figure 7:** UV absorption spectra of  $\text{Fe}_3\text{O}_4$  and  $\text{Fe}_3\text{O}_4/\text{RHA}$ .

**Table 1:** Surface Area of RHA,  $\text{Fe}_3\text{O}_4$ , and  $\text{Fe}_3\text{O}_4/\text{RHA}$ .

S. No	Sample	Crystallite size (nm)	Surface area ( $\text{m}^2/\text{g}$ )
1	RHA	62	145
2	$\text{Fe}_3\text{O}_4$	28	160
3	$\text{Fe}_3\text{O}_4/\text{RHA}$	17	179

### 3.5. UV-Vis Spectrophotometer Measurement of $\text{Fe}_3\text{O}_4$ and $\text{Fe}_3\text{O}_4/\text{RHA}$

Formations of MNPs s of  $\text{Fe}_3\text{O}_4$  and  $\text{Fe}_3\text{O}_4/\text{RHA}$  were detected by spectral analysis under UV-vis spectrophotometer, as shown in Figure 7.

The maximum absorption peaks of both at around 276 nm exhibit excellent magnetic properties suitable for magnetic separation and targeting. An obvious absorption peak appeared between 250 and 300 nm, which indicates the successful impregnated RHA on the surface of magnetic particles. A new absorption band centered at about 320 nm of  $\text{Fe}_3\text{O}_4/\text{RHA}$  can be attributed to the typical electronic transition of an aromatic ring of rice husk ash. The two characteristic absorption spectra ranges at wavelengths of 402 nm and 415 nm indicate the formation of iron nanoparticles [11-13]. This finally brings about oxidations of  $\text{FeSO}_4$ .

### 3.6. Determination of Surface Area

The surface area and crystallite sizes of RHA,  $\text{Fe}_3\text{O}_4$ , and  $\text{Fe}_3\text{O}_4/\text{RHA}$  are presented in Table 1.

A higher surface area is mostly desired over lower surface area for affording high sorption capacity for wastewater treatment and is an important factor that can reveal the adsorption ability of pollutants onto a particles' surface. MNPs s impregnated onto rice husk ash  $\text{Fe}_3\text{O}_4/\text{RHA}$  have large surface area, because carbonyl groups are the main function groups in ash. They decrease with the increasing burning temperature. This phenomenon contributes to the decrease in surface hydroxyl groups. The surface area of rice husk ash depends on the amorphous carbon that is formed during the burning process. Finally, the most important is that the silica layer provides MNPs s with a surface chemically friendly to biological systems.

Crystallinity and verification of available of an oxide in layer structure of  $\text{Fe}_3\text{O}_4$  and  $\text{Fe}_3\text{O}_4/\text{RHA}$  were determined through by XRD. This result presented that some useful mathematical equations for the quantitative determination of in-plane and across plane crystallite sizes, average number of RHA,  $\text{Fe}_3\text{O}_4$ , and  $\text{Fe}_3\text{O}_4/\text{RHA}$  were 62 nm, 28 nm, and 17 nm was calculated by Debye Scherrer equation [7]. Therefore, their average crystallite sizes were negatively related to their surface.

## 4. CONCLUSION

$\text{Fe}_3\text{O}_4$  and  $\text{Fe}_3\text{O}_4/\text{RHA}$  were applied for synthesized using chemical coprecipitation method. Resulted surface areas of RHA,  $\text{Fe}_3\text{O}_4$ , and  $\text{Fe}_3\text{O}_4/\text{RHA}$  were 145, 160, and 179  $\text{m}^2/\text{g}$ , respectively. It was found that on average crystallite size of RHA,  $\text{Fe}_3\text{O}_4$ , and  $\text{Fe}_3\text{O}_4/\text{RHA}$  were 62 nm, 27 nm, and 17 nm. Therefore, their average crystallite sizes were negatively related to their surface areas. SEM results showed that the morphology of  $\text{Fe}_3\text{O}_4$  nanoparticles and its impregnated  $\text{Fe}_3\text{O}_4/\text{RHA}$  homogeneous and uniformly distributed with spherical particles the aggregation of the nanoparticles. From the FT IR spectral data, the absorption bands of RHA,  $\text{Fe}_3\text{O}_4$ , and  $\text{Fe}_3\text{O}_4/\text{RHA}$  the peaks in ( $624$  and  $550$ )  $\text{cm}^{-1}$  are observed corresponding to inherent stretching vibrations of metal-oxygen absorption band (Fe-O bonds) of  $\text{Fe}_3\text{O}_4$ , due to the formation of MNPs s. The main spectrum XRD peak of  $\text{Fe}_3\text{O}_4$  showed at  $2\theta = 35.45^\circ$  (311), in good agreement with the XRD standard for the MNPs ( $\text{Fe}_3\text{O}_4$ ). The spectrum of  $\text{Fe}_3\text{O}_4/\text{RHA}$  was also found as a peak  $2\theta = 22^\circ$  (002) and  $36^\circ$ (311), which indicates silica in crystalline from rice husk ash and retaining of  $\text{Fe}_3\text{O}_4$ . These results confirming that  $\text{Fe}_3\text{O}_4$  and its impregnated onto RHA ( $\text{Fe}_3\text{O}_4/\text{RHA}$ ) were successfully synthesized by coprecipitation method. This research has further attempted to improve the process of environmental application such as industrial application, environmental remediations, and in biomedical application etc.

## 5. ACKNOWLEDGMENTS

The authors Dr Hlaing Hlaing Myint and Khant Nyar Oo are thankful to the Departmental Special Assistance Scheme under the University Grants Commission, and Department of Chemistry, Meiktila University of Myanmar, for financial support and instrumental facilities to continue this research work.

## 6. REFERENCES

- J. Zhou, W. Wu, D. Caruntu, M. H. Yu, A. Martin, J. F. Chen, C. J. O'Connor, W. L. Zhou, (2007) Synthesis and characterization of ultrafine well-dispersed magnetic nanoparticle, *Journal of Physical Chemistry*, **111**(47): 17473-17477.
- S. Liong, (2005) *A Multifunctional Approach to Development, Fabrications and Characterizations of Fe<sub>3</sub>O<sub>4</sub> Composite*, North Ave, Atlanta, Georgia, Georgia Institute of Technology, p213-217.
- G. Oskam, (2006) Metal oxide nanoparticles: Synthesis, characterization and application, *Journal of Sol-Gel Science and Technology*, **37**: 161-164.
- C. P. Lawagon, R. E. C. Amon, (2020) Magnetic rice husk ash 'cleanser' as efficient methylene blue adsorbent, *Environmental Engineering Research*, **25**(5): 685-692.
- G. Sears, (1956) Determination of specific surface area of colloidal Silica by Titration with sodium hydroxide, *Analytical Chemistry*, **28**: 1981-1983.
- P. Scherrer, (1918) Determination of the size and the internal structure of Colloidal Particles by X-rays, *Mathematical Physics Class*, **1918**: 98-100.
- U. Hafeli, W. Schutt, J. Teller, M. Zborowski, (1997) *Scientific and Clinical Applications of Magnetic Microspheres*, New York: Plenum, p324-326.
- F. Adam, S. Balakrishnan, P. L. Wong, (2006) Rice husk ash silica as support material for ruthenium based heterogeneous catalyst, *Journal of Physical Science*, **17**(2): 1-13.
- N. Dehghani, M. Babamoradi, Z. Hajizadeh, A. Maleki, (2020) Improvement of magnetic property of CMC/Fe<sub>3</sub>O<sub>4</sub> nanocomposite by applying external magnetic field during synthesis, *Chemical Methodologies*, **4**(1): 92-99.
- J. A. Lopez, F. González, F. A. Bonilla, G. Zambrano, M. E. Gómez, (2010) synthesis and characterization of Fe<sub>3</sub>O<sub>4</sub> magnetic nanofluid, *Revista Latinoamericana de Metalurgia Y Materiales*, **30**(1): 60-66.
- Y. T. Prabhu, K. V. Rao, B. S. Kumari, V. S. S. Kumar, T. Pavani, (2015) Synthesis of Fe<sub>3</sub>O<sub>4</sub> nanoparticles and its antibacterial application, *International Nano Letters*, **5**(2): 85-92.
- M. Mahdavi, F. Namvar, M. B. Ahmad, R. Mohamad, (2013) Green biosynthesis and characterization of magnetic iron oxide (Fe<sub>3</sub>O<sub>4</sub>) nanoparticles using seaweed (*Sargassum muticum*) aqueous extract, *Molecules*, **18**: 5954-5964.
- S. Mukherjee, S. Paria, (2013) Preparation and stability of nanofluids-a review, *IOSR Journal of Mechanical and Civil Engineering*, **9**: 63-69.
- K. Petcharoen, A.J.M.S. Sirivat, (2012) Synthesis and characterization of magnetite nanoparticles via the chemical coprecipitation method. *Materials Science and Engineering: B*, **177**(5), 421-427.

### \*Bibliographical Sketch



Dr. Hlaing Hlaing Myint is an Associate Professor, Department of Chemistry, Monywa University, Myanmar. Her Doctor of Engineering (D.Eng:) graduated from Department of Transdisciplinary Science and Engineering, Tokyo Institute of Technology (TIT) Japan under the supervision of Prof. Jeffrey S. Cross in 2015. And also, her Post-doctoral Research Fellowship received under the guidance of Prof. Dr. K.S.V. Krishna Rao, Department of Chemistry, Yogi Vemana University, India. Her research interests are in the areas of Chemical engineering, Ionic Liquids, Adsorption Isotherm, Wastewater Treatment, Nanocomposite, Graphene Oxide, Magnetite nanoparticles (Fe<sub>3</sub>O<sub>4</sub>) and Synthesis of Hydrogel. She wrote Abstract book [One book chapter, 2017]. She served as an International Advisory Committee at Thai Institute of Chemical Engineering and Applied Chemistry (TICChE) in 2018. She attended many regional seminars and International Conferences for presenting her research work at Japan 2014, China, 2014, South Korea, 2018, Indonesia 2018, Vietnam 2019, India 2022.



Mr. Aung Phyo Kywae, Demonstrator, Department of Chemistry, Shwebo University, Myanmar. He obtained B.Sc Qualifying Biochemistry from Monywa University in 2018. He completed M.Sc degree under the supervision of Dr. Hlaing Hlaing Myint, Associate Professor, Department of Chemistry, Monywa University, Myanmar in 2022.